

Comparison of Fractal Dimension Estimation Algorithms for Epileptic Seizure Onset Detection

Georgia E. Polychronaki, *Student Member, IEEE*, Periklis Ktonas, *Senior Member, IEEE*, Stylianos Gatzonis, Pantelis A. Asvestas, Eirini Spanou, Anna Siatouni, Hara Tsekou, Damianos Sakas and Konstantina S. Nikita, *Senior Member, IEEE*

Abstract—The fractal dimension (FD) is a natural measure of the irregularity of a curve. In this study the performances of two FD-based methodologies are compared in terms of their ability to detect the onset of epileptic seizures in scalp EEG. The FD algorithms used is Katz’s, which has been broadly utilized in the EEG analysis literature, and the k-nearest neighbor (k-NN), which is applied in this study in a time series sense for the first time. 244.9 hours of EEG recordings, including 16 seizures in 3 patients, were analyzed. Both approaches achieved 100% sensitivity with a false positive rate of 0.85 FP/h for the k-NN algorithm and 1 FP/h for Katz’s algorithm. The corresponding detection delays were 6.5 s and 10.5 s on the average, respectively. The k-NN algorithm seems to outperform Katz’s algorithm. Results are satisfactory in comparison to other methodologies applied on scalp EEG and proposed in the literature.

I. INTRODUCTION

ALTHOUGH computer detection of epileptic seizures is a relatively old field of research, dating in the early 70’s [1], it is still important in the management of epileptic disorders. One issue is that long-term monitoring during pre-surgical evaluation for epilepsy surgery produces huge amounts of electroencephalographic (EEG) recordings which need to be reviewed. For that reason, various automated seizure detection techniques have been developed which aim to detect the presence of a seizure [2]-[7]. A more challenging issue is to develop algorithms for the detection of the onset of epileptic seizures (early detection), with as few false detections as possible. In a hospital setting, this would facilitate prompt medical staff

intervention during seizure activity. Moreover, in an ambulatory setting, seizure onset detection could enable closed-loop stimulation protocols for seizure termination [8]. In both cases, minimization of the false positive (FP) rate (rate of false detections) is important.

Various approaches have been proposed in the literature towards early detection of seizures [9]-[14], most of which have been applied to intracranial EEG recordings [10]-[14], even though routine long-term monitoring as well as ambulatory monitoring usually involve non-invasive scalp EEG [15]. On the other hand, scalp EEG, in comparison to intracranial recordings, is subject to signal attenuation, poor spatial resolution and more noise and artifacts, which make the detection of seizures a more challenging task.

In this study we utilize and compare fractal dimension (FD) estimation algorithms in order to automatically detect the onset of epileptic seizures from long-term scalp EEG recordings acquired during pre-surgical evaluation of patients with refractory mesial temporal lobe epilepsy (MTLE). The term “fractal” can be used to characterize objects in space or fluctuations in time which show a form of self-similarity. The FD is a measure of how complicated a self-similar object is, and in time series analysis it can be used to quantify the irregularity or complexity of a waveform [16].

The FD of EEG has been widely used in the EEG literature [17]- [19], and several FD estimation algorithms have been utilized. Some of the most widely used ones are those proposed by Katz [20], Higuchi [21], and Maragos and Sun [22]. Moreover, different studies have utilized FD methods for the detection of epileptic seizures [5], [13]. Nevertheless, to the best of our knowledge, no extensive study has been published to-date on a FD estimation algorithm applied on multi-day scalp or intracranial EEG. A seizure detection algorithm, which uses a line length measure inspired by Katz’s algorithm, has been presented and evaluated on long-term intracranial EEG data [14].

In this work we compare two FD estimators, with the ultimate goal of real-time epileptic seizure onset detection in long-term continuous scalp EEG. We propose the use of the k-Nearest Neighbor (k-NN) FD estimation algorithm [23] and we compare its performance to that of Katz’s algorithm [20]. To the best

Manuscript received July 5, 2008. The work of G. Polychronaki is supported by the Hellenic State Scholarships Foundation.

G. Polychronaki, E. Spanou and K. Nikita are with the School of Electrical and Computer Engineering, National Technical University of Athens, 9, Heroon Polytechniou Str., Zografou, Athens, 157 80, Greece (corresponding author G. Polychronaki: tel: +30 210 772 2968; fax: +30 210 772 2320; e-mail: gpoly@biosim.ntua.gr).

P. Ktonas is with the Greek Center for Neurosurgical Research “Prof. Petros Kokkalis”, 3, Ploutarxou Str., Athens, 106 75, Greece (e-mail: Periklis.Ktonas@mail.uh.edu).

P. A. Asvestas is with the Department of Medical Instruments Technology, Faculty of Technological Applications, Technological Educational Institute of Athens, Ag. Spyridonos Str., Egaleo, Athens, 122 10, Greece (e-mail: pasv@teiath.gr).

S. Gatzonis, A. Siatouni, H. Tsekou and D. Sakas are with the Epilepsy Surgery Unit, Department of Neurosurgery, University of Athens, “Evangelismos” Hospital, 45-47, Ipsilantou Str., Athens, 106 76, Greece (e-mail: sgatzon@med.uoa.gr).

of our knowledge, this is the first time that the k-NN algorithm is applied in a time series analysis sense, whereas it has been used for image analysis [23]. Moreover, this is the first time that FD methods are evaluated on complete long-term EEG records (including all possible artifacts).

II. MATERIALS AND METHODS

A. Data Description

In this study continuous long-term scalp EEG data from 3 patients with refractory MTLE, containing 16 seizures, were analyzed. All the data were collected in the Epilepsy Telemetry Unit, Department of Neurosurgery, University of Athens, “Evangelismos” Hospital, during long-term video/EEG for pre-surgical evaluation, using a Beehive Millennium Digital Recording System with Grass Telefactor TWin Recording and Analysis Software. Twenty five gold disk electrodes were placed according to the 10-20 system in addition to 6 temporal electrodes (2 of them sphenoidal). After filtering between 0.1 and 70 Hz, data were sampled at 400Hz with 12 bits A/D resolution. A referential electrode montage was used for the analysis, the reference electrode being placed between Cz and Pz. For each patient a standard set of 5 EEG traces was analyzed depending on the lateralization of the seizure origin (T1, T3, T5, F7, 27 for left temporal epilepsy, and T2, T4, T6, F8, 28 for right temporal epilepsy). T1,T2 were placed 3cm below F7, F8, respectively, and 27,28 were placed at mastoidal hilus. Seizure onset times were marked by two independent specialists as the points in time that the first EEG changes occurred which led to a clear seizure discharge.

B. Fractal Dimension Estimation Algorithms

Katz’s Algorithm

Waveforms are collections of points $\vec{p}_i = (x_i, y_i)$ with $x_i < x_{i+1}$, $i=1, 2, \dots, N$ (N : number of points), and are special cases of planar curves. In general, the FD, D , of a planar curve is given by [20]:

$$D = \log(L)/\log(d) \quad (1)$$

where L is the total length of the curve and d its diameter. For waveforms the total length L is the sum of the distances between successive points

$$L = \sum_{i=1}^N \|\vec{p}_{i+1} - \vec{p}_i\|$$

where $\|\cdot\|$ is the Euclidean distance. The diameter (planar extent) d can be considered to be the farthest distance between the starting point and any other point of the waveform:

$$d = \max_i \|\vec{p}_i - \vec{p}_1\|.$$

According to [20] (1) needs to be corrected by making

use of the average step \underline{a} of the waveform, which is the average distance between successive points. Using \underline{a} , (1) becomes:

$$D = \frac{\log(L/\underline{a})}{\log(d/\underline{a})}. \quad (2)$$

Defining n as the number of steps in the curve (one less than the number of points N), then $n = L/\underline{a}$. Substituting n in (2), FD according to Katz’s approach [20] is expressed as:

$$D = \frac{\log(n)}{\log(n) + \log(d/L)}. \quad (3)$$

k-th Nearest Neighbor Algorithm

The k-NN algorithm belongs to a class of algorithms called fixed-mass methods, according to which FD estimation is based on the sizes of cubes which are scaled appropriately as to contain the same number of points (fixed mass) [23] (and references therein). The average distance, $\langle r_k^\gamma \rangle$, of a point from its k-th nearest neighbour can be expressed as a function of k as [24]:

$$\langle r_k^\gamma \rangle = G(k, \gamma) (k/N)^{\gamma/D(\gamma)} \quad (4)$$

where $\gamma = (1-q)D_q$, $D(\gamma) = D_q$, D_q is the multifractal dimension of order q , N is the number of points, and $G(k, \gamma)$ is a function of k and γ , which is near unity for large k . For $q=0$, the fractal dimension is obtained, that is $FD = D_0$ [23], which means that FD is the fixed point of the function $D(\gamma)$, namely $FD = D(FD)$.

The fractal dimension of a waveform is estimated iteratively, using (4), for $k = k_{min}, \dots, k_{max}$ (k integer), as follows [23]:

Step 1: An initial value of γ , i.e. γ_0 , is chosen arbitrarily and $G(k, \gamma)$ is set to unity for every k . Since the fractal dimension of one-dimensional (1D) signals lies theoretically between 1 and 2, it would be better to choose γ_0 in this range, i.e. $\gamma_0 = 1.5$.

Step 2: For every point $\vec{p}_i = (x_i, y_i)$, $i=1, 2, \dots, N$, we calculate the Euclidian distances r_{k_i} from its k nearest neighbors, $k = k_{min}, \dots, k_{max}$.

Step 3: For $j=1, 2, \dots$ the following recursive relations are applied:

$$D(\gamma_j) = \frac{\gamma_{j-1}}{s_{j-1}}, \quad \gamma_j = D(\gamma_j) \quad (5)$$

where s_{j-1} is the slope of the best-fitting line at the points $(\ln(k/N), \ln \langle r_k^{\gamma_{j-1}} \rangle)$ (least squares sense) and

$$\langle r_k^{\gamma_{j-1}} \rangle = \frac{1}{N} \sum_{i=1}^N r_{k_i}^{\gamma_{j-1}}$$

The calculation of (5) is repeated until the quantity

$\left| \frac{D(\gamma_j) - \gamma_{j-1}}{\frac{1}{2}[D(\gamma_j) + \gamma_{j-1}]} \right|$ drops below a certain value (e.g. 10^{-5}) or

a maximum number of iterations is reached (4 in our case). FD is calculated as $D(\gamma_j)$ for the last j .

C. Selection of parameters for FD estimation algorithms

In order to apply the FD estimation algorithms to EEG data, the values of some important parameters must be selected. Those are the length of the sliding window we will use in our analysis (EEG traces will be divided in windows during which FDs will be estimated) and the values of (k_{\min}, k_{\max}) combination to be used for the k-NN FD estimation. Katz's algorithm is free of parameters. Towards this direction, the two algorithms were assessed on synthetic data of known FD (Weierstrass cosine functions [25]) in terms of accuracy and record length N . Moreover, it was examined how the FD estimates using the k-NN algorithm change with (k_{\min}, k_{\max}) in order to select a (k_{\min}, k_{\max}) combination which gives a minimum error between the theoretical and estimated FDs for each particular N examined.

It was found that for $N \geq 800$ the performance of both the Katz and the k-NN algorithm is satisfactory for the whole range of FD values examined (1.1, 1.2, ..., 1.9), with the k-NN algorithm being generally more accurate for all different signal lengths (N) examined. Therefore, for the sliding window analysis in EEG data we chose $N=800$, regarding this value as a good compromise between promoting stationarity in each segment analyzed and having enough data points to ensure reliable estimation of FDs. Moreover, this window length (corresponding to 2sec) is short enough to allow quick detection of seizure onset.

We found that for $N=800$ the combination $(k_{\min}, k_{\max})=(2, 130)$ provided the least error between the theoretical and estimated FDs. Therefore, we used this value for our EEG analysis.

D. Description of seizure onset detection procedure

Analysis of EEG was performed on the full recording of each patient (including night sleep). No pre-selection of data was undertaken in order to exclude artifacts such as those introduced by electromyographic (EMG) activity during chewing, movement of the patient or electrode failure. A FP was defined as any non-seizure event that was detected by the system. Duration of recordings in hours is shown in Table I.

The first step of our approach included band pass filtering of the data between 3-30Hz. The reason for this was three-fold: a) seizure activity lies more often between 3 and 29Hz [2] b) occurrences of 0-3 Hz activity can be frequent in non-ictal sleep EEG and c) this filtering removed high amplitude slow post-ictal EEG activity which in our analysis proved to be the cause of a great number of FP (which were eliminated after filtering). A zero-phase Butterworth filter of order 4 was used. After filtering, a sliding window approach was used

for further analysis: 2s-length windows (corresponding to 800 points) with no overlap were used, as explained before. As a second step of our approach, the variance of each data window was computed and the EEG values of each data window were divided by the corresponding variance value. The motivation behind this action will be explained later in this section.

After following the aforementioned procedure, new time series were produced, points of which corresponded to FD estimations for each data window. From the resulting time series it became clear (see Fig. 1) that FD dropped during seizures in most cases. A threshold was applied to determine the detection status of each window: if the FD value of a given window was below the threshold value, then that window was candidate of being the start of a seizure. Towards this direction, a parameter w was defined as the number of FD values (number of windows) that should have remained under the threshold in order for the last window to be characterized as "detection" (the procedure for threshold selection is explained later in this section). This was done in order to avoid producing detections due to short bursts of activity or short artifacts. In the present study we used $w=2$. Detections separated by less than 40 sec were grouped and counted as a single detection (similar approach to [9]). A detection delay was defined as the time elapsed between the beginning of a seizure as defined by the EEG specialists and the end of the first window detected in the sense described above.

Since the pattern we wanted to detect was a drop in the FD time series that could be indicative of a seizure, it would be desirable to find ways to make the seizure and the non-seizure EEG states more distinguishable in terms of FDs. The action of dividing the EEG values of each window with their variance was towards that end. The variance of the EEG of a window usually gets larger when a seizure occurs (as found in this work and mentioned in [6]). Dividing the EEG values of a window with their variance resulted in lowering the EEG values during seizure windows in comparison to non-seizure ones. Due to the amplitude dependence of FD estimation algorithms in this work (e.g., see [26]), this meant estimation of comparatively lower FDs during seizures. This led to fewer FPs and smaller detection delays.

One important issue was the selection of the threshold. In this work we adopted a user tunability operation similar to the one proposed in [9], which allows the user to make the choice of sacrificing seizure detections (or having bigger delays) by changing the threshold value in order to reduce high FP rates. Thus we defined a range of threshold values for the user to choose from as follows: after producing the FD time series from our EEG data, we tried different threshold values for both Katz and k-NN algorithms. For each method we found a range of threshold values which included, for all the patients, an optimum threshold. The optimum threshold was defined

TABLE I
COMPARATIVE RESULTS OF KATZ AND K-NN ALGORITHMS WITH OPTIMUM THRESHOLD VALUES

Patient	Number of Seizures	Duration of Recording (h)	k-NN Algorithm			Katz Algorithm				
			Optimum Threshold	True Positives (%)	FP/h	Mean Detection Delay (s)	Optimum Threshold	True Positives (%)	FP/h	Mean Detection Delay (s)
1	4	13	1.26	100	0.23	6.5	1.15	100	0.61	10.5
2	5	164	1.21	100	1.42	5.8	1.12	100	1.41	6.6
3	7	67.9	1.22	100	0.91	18.4	1.13	100	0.99	27.8
Total				mean	mean	median		mean	mean	median
				100	0.85	6.5		100	1.00	10.5

as the lowest threshold for which 100% sensitivity with as small detection delays as possible was achieved, and which at the same time produced the lowest number of FPs. In most cases, FP rates for this optimum threshold were comparable to the ones reported in the literature, i.e. less than 1FP/h. We did not allow FP rates greater than 1.5 FP/h ([7] reports 1.35 FP/h). The range of threshold values defined in this work is 1.11-1.16 for Katz-based results and 1.21-1.26 for k-NN-based results, with step 0.1 (we selected 6 threshold values for both algorithms). As default threshold value one could use 1.11 for Katz and 1.21 for k-NN algorithms.

III. RESULTS

The results for optimum threshold values for each method are shown in Table I. For patients 1 and 3 both algorithms achieved less than 1FP/h. For patient 2 this was not the case, as for this patient the recording was quite long and the quality of the recording started deteriorating significantly during the fourth day: the FP rate was 0.56 FP/h for the first 90 hours of the recording and 2.47 FP/h for the rest 74 hours using the k-NN algorithm and 0.61 FP/h and 2.39 FP/h using Katz's algorithm (for the threshold values of Table I).

All results presented in Table I correspond to the best channel out of the 5 analyzed in the sense of having the minimum detection delays in combination with the minimum number of FPs. These channels are T5, T2, and 28 for patients 1, 2, and 3, respectively.

Fig. 1 shows FD time series produced from patients 1 and 2. We notice there is a clear drop of FD values during each seizure, while the FD values return to their pre-ictal level immediately after the end of the seizure in most cases. Reference electrode failure and EMG activity caused by chewing were the main cause of false positives in our system.

An example of false detections is shown in Fig. 1, for seizure 4, patient 2. In this case there exist two additional vertical dashed lines after the end of the seizure, in both Katz and k-NN methods. These correspond to FPs produced by our method due to poor EEG quality (reference electrode failure). Fig. 2 shows the part of EEG corresponding to the first false detection mentioned above. This FP was produced by the four seconds of EEG which start from the bold vertical line (two 2 s windows).



Fig. 2. False detection from patient 2 caused by reference electrode failure. Solid vertical line indicates the start of the 4 sec interval which caused the false detection. Light vertical lines indicate 1 s intervals.

Table II shows the detection delays for all seizures of all patients. It is worth mentioning that of all seizure detections, 93.75% using the k-NN method and 81.25% using Katz's method were achieved within the first one third of the corresponding seizure duration.

IV. DISCUSSION

Our approach is designed with ultimate goal to be appropriate for on-line EEG analysis (real-time prospective analysis). It is general as it does not require any prior information about the signal analyzed and it does not depend on pattern recognition as other works in the seizure detection literature do [7].

Comparison of results (Table I and Table II) for the two applied methods shows that the proposed k-NN algorithm seems to perform better than Katz's; it achieves a shorter median detection delay (6.5s) in comparison to Katz's (10.5s), while at the same time it produces less FPs (0.85FP/h) in comparison to Katz's (1.00FP/h).

TABLE II
COMPARATIVE RESULTS OF KATZ AND K-NN ALGORITHMS WITH OPTIMUM THRESHOLD VALUES: DELAYS (S) OF DETECTIONS FOR EACH SEIZURE

Patient	Seizure number							median
	1	2	3	4	5	6	7	
k-NN Algorithm								
1	7	5	7	7				7
2	8	5	7	4	5			5
3	12	11	59	7	7	27	6	11
Katz's Algorithm								
1	23	5	7	7				7
2	8	5	9	6	5			6
3	12	11	57	39	43	27	6	27

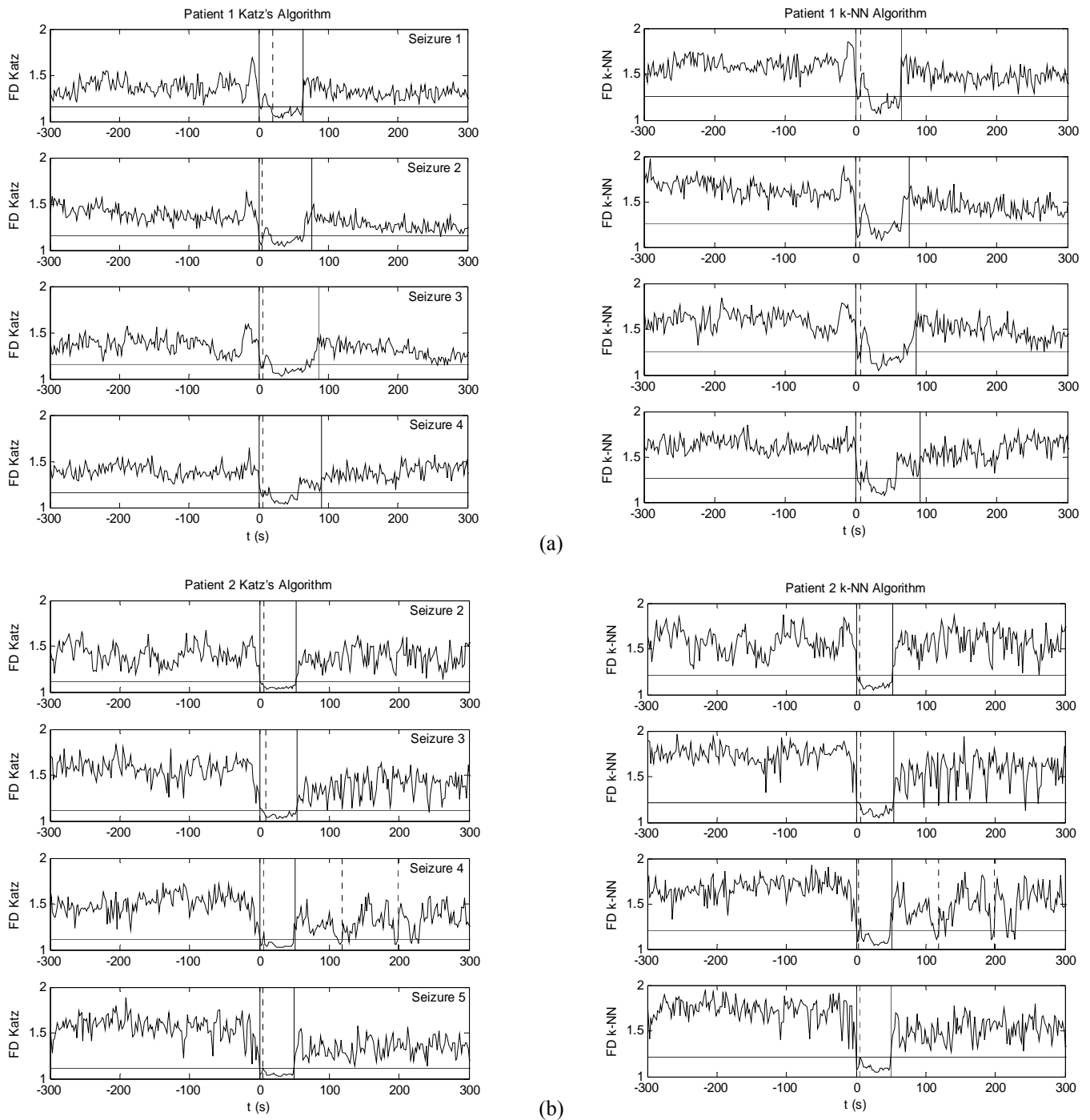


Fig. 1. FD estimations using Katz and k-NN algorithms. Time $t=0$ corresponds to the seizure onset time while 5 minutes before and after the seizure onset are shown. Vertical solid lines indicate the beginning and the end of a seizure. Vertical dashed lines indicate times of detections. Horizontal lines indicate the optimum threshold values for each patient. Detections separated by less than 40 sec are grouped and counted as a single detection. (a) Patient 1, all seizures (b) Patient 2, seizures 2-5

Maybe this difference exists due to the better estimation accuracy of the k-NN algorithm which we found during the analysis of synthetic data. Analysis of more EEG records is required in order to further test the superiority of the k-NN algorithm.

As mentioned in the introduction, although there exists enough literature on seizure onset detection, most of the work has been done using intracranial recordings. Due to

the very different nature of scalp and intracranial EEG, we can only compare the results of the present study to those of studies based on scalp EEG [7], [9]. The system of Saab and Gotman [9] aims to detect the onset of epileptic seizures in scalp EEG, based on wavelet decomposition and Bayesian probabilities. Using the tuning mechanism mentioned before, they reported 76% sensitivity, a FP rate of 0.34FP/h and a median detection

delay of 10 s (ideal threshold results) after analysis of 360 h of scalp EEG, which included 69 seizures in 16 patients. In our study we achieved a perfect sensitivity and similar or better delays to [9], but our results cannot be directly compared to theirs due to the fact that we only used seizures from MTL patients.

The FP rates reported in [9] are achieved only after the alpha EEG rhythm, EMG and electrode failure artifacts are (automatically) taken account of. On the other hand, the false positive rates reported in our study are “raw” results, in the sense that no artifact removal procedures were performed. Therefore, again, our results cannot be directly compared to [9]. We expect a great reduction of false positives by applying automatic artifact reduction methods particularly aimed at the removal of reference electrode failure and EMG activity caused by chewing artifacts. We noticed that those two types of artifacts were the main cause of false positives in our system. Important is the fact that, comparatively, we did not have large number of FPs originating from patterns such as alpha EEG activity, rapid eye blinking or short bursts of rhythmic EEG activity, in contrast to [9].

On the other hand, Gabor in [7] reported 92.8% sensitivity and 1.35 ± 1.35 FP/h using 4553.8 h of scalp EEG, which included 181 seizures from 65 patients; detection delays were not reported, as this study emphasized seizure identification and not seizure onset detection. Our method, tested on a limited number of patients, seems to outperform both their sensitivity (overall) and their FP rate for 2 out of 3 patients analyzed. In future work, application of our method to EEG data from more patients is needed in order for comparisons with other methods to become more appropriate. Moreover, more epilepsy types (having different seizure characteristics) should be included in the analysis. Finally, in the future we could use clear separation of testing and training data for threshold selection.

REFERENCES

[1] J. R. Ives, C. J. Thompson, P. Gloor, A. Olivier, and J. F. Woods, “The on-line computer detection and recording of spontaneous temporal lobe epileptic seizures from patients with implanted depth electrodes via a radio telemetry link”, *Electroen Clin Neuro*, vol. 37, pp. 205, 1974

[2] J. Gotman, “Automatic recognition of epileptic seizures in the EEG”, *Electroen Clin Neuro*, vol. 54, pp. 530-540, 1982

[3] J. Gotman, “Automatic seizure detection: improvements and evaluation”, *Electroen Clin Neuro*, vol. 76, pp. 317-324, 1990

[4] A. M. Murro, D. W. King, J. R. Smith, B. B. Gallagher, H. F. Flanigin and K. Meador, “Computerized seizure detection of complex partial seizures”, *Electroen Clin Neuro*, vol. 79, pp. 330-333, 1991

[5] E. T. Bullmore, M. J. Brammer, P. Bourlon, G. Alarcon, C. E. Polkey, R. Elwes, and C. D. Binnie, “Fractal analysis of electroencephalographic signals intracerebrally recorded during 35 epileptic seizures: evaluation of a new method for synoptic visualization of ictal events”, *Electroen Clin Neuro*, vol. 91, pp. 337-345, 1994

[6] P. E. McSharry, T. He, L. A. Smith, and L. Tarassenko, “Linear and non-linear methods for automatic seizure detection in scalp

electro-encephalogram recordings”, *Med Biol Eng Comput*, vol. 40, pp. 447-461, 2002

[7] A. J. Gabor, “Seizure detection using a self-organizing neural network: validation and comparison with other detection studies”, *Electroen Clin Neuro*, vol. 107, pp. 27-32, 1998

[8] W. H. Theodore and R. S. Fisher, “Brain stimulation for epilepsy”, *Lancet Neurol*, vol. 3, pp. 111-118, 2004

[9] M. E. Saab and J. Gotman, “A system to detect the onset of epileptic seizures in scalp EEG”, *Clin Neurophysiol*, vol. 16, no. 2, pp. 427-442, 2005

[10] S. Grewal and J. Gotman, “An automatic warning system for epileptic seizures recorded on intracerebral EEGs”, *Clin Neurophysiol*, vol. 116, no. 10, pp. 2460-2472, 2005

[11] I. Osorio, M. G. Frei, and S. B. Wilkinson, “Real-time automated detection and quantitative analysis of seizures and short-term prediction of clinical onset”, *Epilepsia*, vol. 36, no. 6, pp. 615-627, 1998

[12] I. Osorio, M. G. Frei, J. Giftakis, *et al*, “Performance reassessment of a real-time seizure-detection algorithm on long ECoG series”, *Epilepsia*, vol. 43, no. 12, pp. 1522-1535, 2002

[13] R. Esteller, G. Vachtsevanos, J. Echauz, T. Henry, P. Pennell, C. Epstein, R. Bakay, C. Bowen, and B. Litt, “Fractal dimension characterizes seizure onset in epileptic patients”, *Proc Int Conf ASSP*, Phoenix, USA, vol. 4, pp. 2343-2346, 1999

[14] R. Esteller, J. Echauz, T. Tchong, B. Litt, and B. Pless, “Line length: an efficient feature for seizure onset detection”, *Proc 23rd Annu EMBS Int Conf*, Istanbul, Turkey, pp. 1707-1710, 2001

[15] W. O. Tatum IV, L. Winters, M. Gieron, *et al*, “Outpatient Seizure Identification: Results of 502 patients using computer-assisted ambulatory EEG”, *Clin Neurophysiol*, vol. 16, no. 2, pp. 427-442, 2005

[16] M. J. Katz and E. B. George, “Fractals and the analysis of growth paths”, *B Math Biol*, vol. 47, no. 2, pp. 273-286, 1985

[17] R. Esteller, G. Vachtsevanos, J. Echauz, and B. Litt, “A comparison of waveform fractal dimension algorithms”, *IEEE Trans Circuits Syst - I: Fundamental Theory and Applications*, vol. 48, no. 2, pp. 177-183, 2001.

[18] J. E. Arle and R. H. Simon, “An application of fractal dimension to the detection of transients in the electroencephalogram”, *Electroen Clin Neuro*, vol. 75, pp. 296-305, 1990

[19] A. Accardo, M. Affinito, M. Carrozzini, and F. Bouquet, “Use of the fractal dimension for the analysis of electroencephalographic time series”, *Biol Cybern*, vol. 77, pp. 339-350, 1997

[20] M. J. Katz, “Fractals and the analysis of waveforms”, *Comput Biol Med*, vol. 18, no. 3, pp. 145-156, 1988

[21] T. Higuchi, “Approach to an irregular time series on the basis of the fractal theory”, *Physica D*, vol. 31, pp. 277-283, 1988

[22] P. Maragos and F. K. Sun, “Measuring the fractal dimension of signals: morphological covers and iterative optimization”, *IEEE T Signal Proces*, vol. 41, no. 1, 1993

[23] P. Asvestas, G. K. Matsopoulos, and K. S. Nikita, “Estimation of fractal dimension of images using a fixed mass approach”, *Pattern Recogn Lett*, vol. 20, no. 3, pp. 347-354, 1999

[24] P. Grassberger, “Generalizations of the Hausdorff dimension of fractal measures”, *Phys Lett*, 107A, 101-105

[25] C. Tricot, *Curves and Fractal Dimension*, New York: Springer-Verlag, 1995

[26] A. Ripoli, A. Belardinelli and R. Bedini, “An effective algorithm for quick fractal analysis of movement biosignals in ambulatory monitoring”, *Proc 20th Annu EMBS Int Conf*, Hong Kong, China, vol. 20, no. 3, pp. 1591-1594, 1998